© 2015. Published by The Company of Biologists Ltd | Development (2015) 142, 1705-1716 doi:10.1242/dev.117879

RESEARCH ARTICLE

Sperm-inherited organelle clearance in *C. elegans* relies on LC3-dependent autophagosome targeting to the pericentrosomal area

Abderazak Djeddi[1,2], Sara Al Rawi[1,2], Jane Lynda Deuve[1,2], Charlene Perrois[1,2], Yu-Yu Liu[1,2], Marion Russeau[1,2], Martin Sachse[3] and Vincent Galy[1,2,*]

ABSTRACT

Macroautophagic degradation of sperm-inherited organelles prevents paternal mitochondrial DNA transmission in *C. elegans*. The recruitment of autophagy markers around sperm mitochondria has also been observed in mouse and fly embryos but their role in degradation is debated. Both worm Atg8 ubiquitin-like proteins, LGG-1/GABARAP and LGG-2/LC3, are recruited around sperm organelles after fertilization. Whereas LGG-1 depletion affects autophagosome function, stabilizes the substrates and is lethal, we demonstrate that LGG-2 is dispensable for autophagosome formation but participates in their microtubule-dependent transport toward the pericentrosomal area prior to acidification. In the absence of LGG-2, autophagosomes and their substrates remain clustered at the cell cortex, away from the centrosomes and their associated lysosomes. Thus, the clearance of sperm organelles is delayed and their segregation between blastomeres prevented. This allowed us to reveal a role of the RAB-5/RAB-7 GTPases in autophagosome formation. In conclusion, the major contribution of LGG-2 in sperm-inherited organelle clearance resides in its capacity to mediate the retrograde transport of autophagosomes rather than their fusion with acidic compartments: a potential key function of LC3 in controlling the fate of sperm mitochondria in other species.

KEY WORDS: LC3, LGG-2, Allophagy, Autophagy, Fertilization, MtDNA transmission

INTRODUCTION

Maternal inheritance of mitochondrial genome occurs in most animal species and requires the elimination of paternal contribution around fertilization time. This is achieved by different means, including sperm mitochondrial DNA (mtDNA) destruction prior to gamete fusion, physical degradation and/or exclusion of the sperm mitochondria and/or of their nucleoids, as well as the segregation of these mitochondria in specific tissues such as extra-embryonic ones (Luo et al., 2013b). In several species, sperm entry triggers the formation of allophagosomes via the local recruitment of proteins of the macroautophagy machinery. Whereas their active role in sperm-inherited organelle degradation is clear for *C. elegans* and *D. melanogaster* (Al Rawi et al., 2011; Politi et al., 2014; Sato and Sato, 2011; Zhou et al., 2011), it is still debated for mammalian embryos (Luo et al., 2013a).

[1]Sorbonne Universités, UPMC, Univ Paris 06, Institut de Biologie Paris-Seine (IBPS), UMR7622, Paris F-75005, France. [2]CNRS, IBPS, UMR7622, Paris F-75005, France. [3]PFMU, Imagopole, Institut Pasteur, Paris F-75015, France.

*Author for correspondence (vgaly@snv.jussieu.fr)

Received 16 September 2014; Accepted 16 March 2015

Macroautophagy (henceforth termed 'autophagy') is an intracellular catabolic process involving the formation around the substrates of double-membrane compartments called autophagosomes, or allophagosomes in the case of sperm organelles clearance. Autophagosome biogenesis is mediated by autophagy-related (ATG) proteins (reviewed by Mizushima et al., 2011). Members of the Atg8p family are ubiquitin-like proteins responsible for expansion of the autophagosomal membranes, membrane tethering and hemifusion evoked by the conjugation with phosphatidylethanolamine (PE) (Nakatogawa et al., 2007), and their anchoring to the membranes of the phagophores. Whereas yeast has a single Atg8p protein, mammals have seven, in two subfamilies. The first subfamily consists of the MAP1LC3 (microtubule-associated protein 1 light chain 3, hereafter referred to as LC3) proteins, with LC3A as the most prevalent and established autophagosome marker. The second subfamily consists of the GABARAP proteins.

Addressing the function of LC3 in allophagosomes maturation is important in the light of recent studies showing the recruitment of autophagy markers around sperm-inherited mitochondria in mouse (Al Rawi et al., 2011; Luo et al., 2013a) and in *Drosophila* (Politi et al., 2014) embryos. This has led to conclusions ranging from the non-involvement of autophagy in the degradation of the paternal mitochondria to a role in a non-canonical autophagy involving the endosomal pathway. In mouse embryos, GFP-LC3 disappeared before the clearance of labeled sperm mitochondria, suggesting that LC3 was not involved in their autophagy degradation (Luo et al., 2013a). Furthermore, the conditional knockout of *Atg5*, preventing the coupling of LC3 proteins to the PE anchor, did not dramatically modify the fate and distribution of sperm mitochondria in the embryos (Luo et al., 2013a). These findings suggested that, despite the evolutionarily conserved recruitment of the autophagy markers around sperm-inherited mitochondria, they might not always be involved in their autophagy degradation. Interestingly, mouse paternal mitochondria tend to remain clustered and are transmitted to a limited number of daughter cells, with a bias toward the blastomeres forming the future extra-embryonic tissue. This unknown mechanism coupled to the reduction of mtDNA in the spermatozoa would contribute to the elimination of the sperm mtDNA from the embryo (Luo et al., 2013a)

In *C. elegans* embryos, autophagy is required for sperm-inherited organelle degradation, including the mitochondria and their genome (Al Rawi et al., 2011; Sato and Sato, 2011; Zhou et al., 2011). Both LGG-1 (GABARAP) and LGG-2 (LC3) are localized in the allophagosomes formed around sperm-inherited mitochondria and the nematode-specific sperm membranous organelles (MO) after fertilization (Al Rawi et al., 2011; Sato and Sato, 2011), suggesting their implication in the degradation of sperm-inherited components.

Development (2015) 142, 1705-1716 doi:10.1242/dev.117879

Transmission electron microscopy (TEM) and immunogold labeling confirmed that GFP-tagged LGG-1 and LGG-2 are present in autophagosomes (Manil-Ségalen et al., 2014). *lgg-1(tm3489)* null mutants are sterile and fail to degrade sperm-inherited organelles as well as sperm-inherited mtDNA (Al Rawi et al., 2011; Sato and Sato, 2011). LGG-2 RNAi depletion reduced the viability of the dauer (a stage of developmental arrest) worms and the lifespan of the adults (Alberti et al., 2010). LGG-2 RNAi treatment was lethal in mutants carrying a loss-of-function mutation in *daf-2*, the *C. elegans* insulin-like tyrosine kinase receptor that triggers constitutive dauer entry (Meléndez et al., 2003). Furthermore, LGG-2-depleted embryos accumulate P-granule components in the somatic cells (Zhang et al., 2009). In *lgg-2(tm5755)* mutant embryos, LGG-1 was still recruited around sperm organelles and appeared clustered in the early embryos (Manil-Ségalen et al., 2014). This striking clustering phenotype was proposed to be a consequence of a defect in autophagosome acidification (Manil-Ségalen et al., 2014), a function that would be mediated via LGG-2 interaction with VPS-39 (Manil-Ségalen et al., 2014). The potential link with the endosomal pathway was intriguing and could be conserved among species, as suggested by the localization of VPS-27 in potential hybrid compartments between endosomes and autophagosomes (amphisomes) around sperm-inherited organelles in one-cell-stage *C. elegans* embryos (Manil-Ségalen et al., 2014) as well as the colocalization of Rab7 with sperm mitochondria in *Drosophila* embryos (Politi et al., 2014).

An essential step during the degradation of autophagy substrates is the formation of autolysosomes upon fusion between the autophagosomes and the lysosomes (Tanida et al., 2005) and the activation of hydrolases upon acidification (Sun-Wada et al., 2009). Interestingly, $LC3^+$ autophagosomes were associated with microtubules during autophagosome formation or maturation and were required for bringing autophagosomes and lysosomes or endosomes together prior to fusion and disposal of the cargos (Fass et al., 2006; Köchl et al., 2006). In primary neurons, the $LC3^+$ autophagosomes were also maturing during their microtubule-dependent transport toward the cell soma (Maday et al., 2012) but LC3 role in the process remained unclear. The microtubule-dependent transport of autophagosomes was inhibited using anti-LC3 antibodies in HeLa cells (Kimura et al., 2008).

As *lgg-2(tm5755)* worms were viable, LGG-2 function in acidification appeared not essential. Furthermore, the impact of *lgg-2* mutation on the efficiency of substrate degradation was not quantified (Manil-Ségalen et al., 2014). We therefore tested whether LGG-2 could indeed act in facilitating acidification of the autophagosomes by controlling their cellular distribution rather than by allowing their fusion itself. Taking advantage of the stereotyped *C. elegans* early embryogenesis we characterized the fate and dynamics of the allophagosomes by tracking endogenous autophagy proteins, as well as sperm-organelles in wild-type and *lgg-2* null mutant embryos. We show that, if LGG-2 is not required for the formation of closed $LGG\text{-}1^+$ autophagosomes, it is crucial for their normal spatial distribution and dynamics in the early dividing zygote. We demonstrate that the retrograde migration of the substrates toward the centrosomes requires their entry in autophagosomes, LGG-2, astral microtubules and Dynein heavy chain (DHC-1), whereas it occurs independently of the acidification of the allophagosomes. In addition, we provide evidence that, whereas RAB-5 is essential in an early step of allophagosome formation, LGG-2 is required for $RAB\text{-}7^+$ structure distribution and acidification. In summary, our study reveals that the spatial distribution and the efficient degradation of sperm-inherited components after fertilization are functionally connected and dependent on LGG-2/LC3, a property that might be conserved in other species and could participate in the elimination of paternal mitochondrial genome in the embryo.

RESULTS

The persistence of clustered allophagosomes in *C. elegans* embryos lacking the LGG-2 protein is coupled to a delayed clearance of sperm mitochondria and membranous organelles

Both *C. elegans* orthologs of Atg8p, LGG-1 and LGG-2, were localized in membranous compartment-like structures at the embryonic posterior pole around sperm mitochondria (100%, n=21) (Al Rawi et al., 2011; Sato and Sato, 2011; see also supplementary material Fig. S1A). Recently, based on the characterization of the *lgg-2(tm5755)* embryos, it has been proposed that LGG-2 was required for allophagosome acidification via its interaction with VPS-39 (Manil-Ségalen et al., 2014) and would be responsible for the clustering phenotype of the allophagosomes. Intriguingly, a correlation between a potential defect in acidification and a defect in substrate degradation was missing, and it was not addressed how the absence of LGG-2 could trigger the strong defect in allophagosome spatial distribution. We therefore tested the impact of the loss of LGG-2 on substrates degradation, allophagosome acidification and their dynamics.

In order to confirm that the abnormal localization of the allophagosomes is caused by the absence of full-length LGG-2, we characterized a second viable mutant allele with a deletion within the ORF of *lgg-2*: *lgg-2(tm6474)*. Using RT-qPCR analysis on total RNA extracts we confirmed the nature of the deletion and the absence of *lgg-2* full-length RNA molecules in both *lgg-2* mutants (supplementary material Fig. S2A). We also observed the absence of detectable LGG-2 signal in *lgg-2(tm6474)* embryos, confirming that it is probably a null allele (supplementary material Fig. S1B). Importantly, in the absence of LGG-2-specific signal in *lgg-2(tm6474)* embryos, LGG-1 was still recruited at the posterior pole and at the normal time (100%, n=13), and remained clustered (100%, n=23) (supplementary material Fig. S1B and Fig. S2B), demonstrating that the persistent clustering phenotype is linked to the absence of detectable LGG-2 protein.

In order to confirm that the clustered $LGG\text{-}1^+$ structures are allophagosomes and to evaluate whether the lack of dispersion and the persistence of the $LGG\text{-}1^+$ structures in the *lgg-2(tm5755)* embryos could be due to a block in the process of allophagosome maturation, we examined an early two-cell-stage *lgg-2(tm5755)* embryo by TEM and systematic serial sectioning (Fig. 1A-D). We found autophagosomal structures in a single region of the embryos, away from the nuclei (Fig. 1A,B). The allophagosomes were correctly formed and contained intact or partially degraded mitochondria, which were unequivocally identified by the presence of their inner and outer membrane (Fig. 1B-D). The allophagosomes were characterized by two delimiting membranes visible at high magnification (Fig. 1C,D).

We then tested whether LGG-1 is required to maintain the cluster of allophagy substrates observed in the absence of LGG-2. We labeled sperm mitochondria (Fig. 1E) and MO (supplementary material Fig. S3A,B) in control *lgg-2(tm5755)* embryos or additionally RNAi-depleted for LGG-1. We observed that, as in the *lgg-2(tm5755)* embryos, sperm mitochondria (100%, n=13) and MO (100%, n=5) were normally localized around sperm DNA in meiosis II embryos in the absence of both

Development (2015) 142, 1705-1716 doi:10.1242/dev.117879

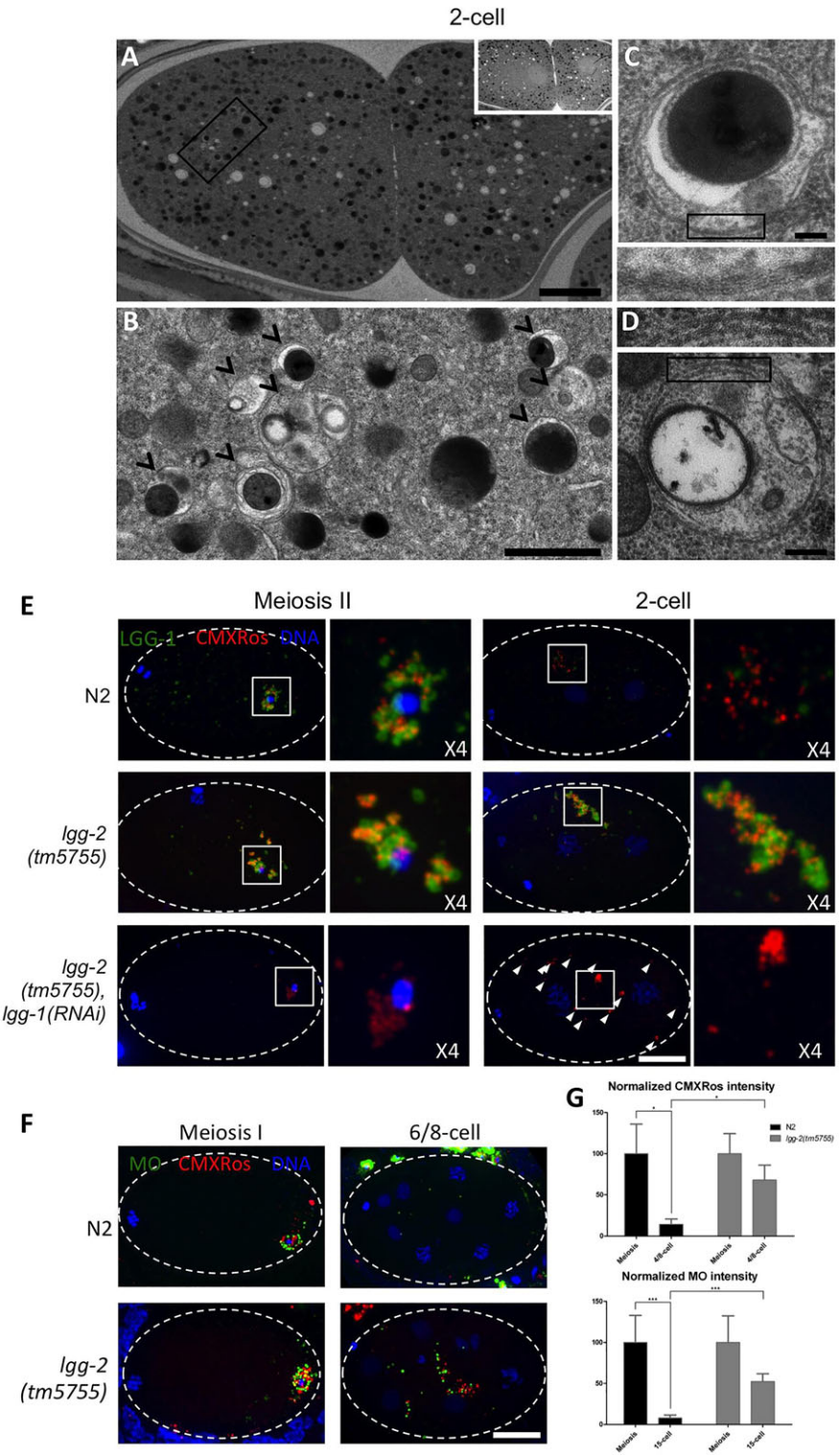

Fig. 1. The clearance of sperm mitochondria and nematode-specific membranous organelles is delayed in the absence of LGG-2. (A-D) Transmission electron micrographs of an early two-cell-stage *lgg-2(tm5755)* embryo. Allophagosomes containing mitochondria are concentrated in a peripheral region (A,B) 6 µm away from the two nuclei (inset in A). Intact (C) or partially degraded mitochondria (D) are found in allophagosomes delimitated by two membranes (zoom). (E) Maximum-intensity *z*-projections (MIP) of confocal images of wild-type (N2), *lgg-2(tm5755)* and *lgg-2(tm5755);lgg-1(RNAi)* embryos stained for LGG-1 (green), mitotracker-labeled sperm mitochondria (red), DNA (blue) and fourfold magnified views of the highlighted areas. (F) MIP of confocal images showing labeled sperm mitochondria (red) and nematode-specific membranous organelles (MO, green) in wild-type (N2, top panels) versus *lgg-2(tm5755)* embryos (bottom panels). (G) Quantification of normalized intensities of sperm mitochondria and MO at the specific stages in wild type compared with *lgg-2 (tm5755)*. Data are shown as mean±s.e.m. with the following statistical significance: **P*<0.05, ****P*<0.001. Scale bars: 10 µm in E,F; 5 µm in A; 1 µm in B; 100 nm in C; 200 nm in D.

LGG-1 and LGG-2 proteins (Fig. 1E and supplementary material Fig. S3B). Whereas, by the two-cell stage, the MO (100%, *n*=18) (supplementary material Fig. S3A,B) and sperm mitochondria (100%, *n*=32) (Fig. 1E) were associated with LGG-1 signal aggregated and restricted to a small area in the periphery of *lgg-2 (tm5755)* embryos, the LGG-1 signal was absent and the sperm-inherited organelles were no longer aggregated in the *lgg-2 (tm5755)* embryos treated with *lgg-1(RNAi)* (100%, *n*=18 for MO; 100%, *n*=11 for sperm mitochondria) (Fig. 1E and supplementary material Fig. S3B). In order to strengthen the conclusion that LGG-2 functions in allophagosomes rather than in isolated substrates, we tested the impact of interfering with the ubiquitin-like conjugating machinery. Upon RNAi depletion of the ATG-5 (*n*=13) and ATG-7 proteins (*n*=22) and in *atg-3 (bp412)* mutant embryos (*n*=30), a complete absence of LGG-2 recruitment around the allophagy substrates was observed

Development (2015) 142, 1705-1716 doi:10.1242/dev.117879

(supplementary material Fig. S1C). These data demonstrate that the persistent clustering of sperm-inherited allophagy substrates in the absence of LGG-2 requires LGG-1 and their entry in LGG-1^{+} allophagosomes.

In order to test whether the lack of dispersion of allophagosomes in *lgg-2* mutant embryos compromises their catabolic activity, we measured the kinetics of sperm organelle degradation. As in the wild-type meiosis I embryos, sperm mitochondria and MO were localized at the posterior pole close to the sperm DNA in *lgg-2 (tm5755)* embryos (Fig. 1F). In both cases, the allophagy substrates were absent after the 100-cell stage, whereas, in the earlier stages of development, we detected the persistence of the substrates in the *lgg-2(tm5755)* embryos (Fig. 1F). Allophagy substrates were quantified by measuring the fluorescent signal intensity of MO and sperm mitochondria in wild-type and *lgg-2 (tm5755)*-fixed embryos. We revealed the stabilization of the fluorescent structures in four- to eight-cell-stage embryos, with 58.3±17.4% (s.e.m.) of the mean intensity left in the *lgg-2 (tm5755)* (n=9) versus 14.1±6.5% left in the N2 (n=9) for the sperm mitochondria, and in 15-cell-stage embryos, with 52.5±9.4% of the mean intensity left in the *lgg-2(tm5755)* (n=10) versus 7.8±3.7% left in the N2 (n=8) for the MO (Fig. 1G). Therefore, we concluded that the persistent clustering observed in the absence of LGG-2 is correlated with a delay in the clearance of sperm-inherited organelles.

The spatial distribution of sperm-inherited allophagy substrates depends on microtubule-organizing center movement during the first embryonic divisions

The cellular events, after fertilization in *C. elegans* embryos, follow a highly reproducible pattern allowing the characterization of abnormal early embryo development (Hird and White, 1993; Sönnichsen et al., 2005). We therefore characterized the dynamics of the allophagosome substrates during the first zygotic cell divisions in order to clarify the contribution of LGG-2. We followed the movement of mitotracker-labeled sperm-inherited mitochondria in control embryos using live confocal microscopy (Fig. 2A). Upon fertilization, sperm mitochondria flowed into the ooplasm and remained mostly grouped around paternal nuclear DNA at the posterior pole until the end of the second meiotic division (Fig. 2A and supplementary material Movie 1). After meiosis, while the female and the male pronuclei formed at each pole of the embryo (Fig. 2A and supplementary material Movie 1), the sperm mitochondria were pushed into the posterior cortical region (Fig. 2A and supplementary material Movie 1). Then, they moved along the cortex toward the anterior pole of the embryo. When the female pronucleus was attracted by the male pronucleus and the astral microtubules emanating from the two centrosomes, the sperm-inherited mitochondria were gathered around the two centrosomes and followed the movement of the centrosomes/pronuclei complex, while it was centered and rotated in the embryo prior to the first mitotic division (75%, n=14) (Fig. 2A and supplementary material Movie 1). The peculiar dynamics of the sperm mitochondria suggested a link with mitotic microtubules organized by the microtubule-organizing center (MTOC). We extended our observation to the MO, using a strain expressing the sperm protein PEEL-1 fused to GFP (Seidel et al., 2011). GFP::PEEL-1 was observed as structures around sperm DNA after fertilization and colocalized with the MO detected using the SP56 antibody on fixed embryos (supplementary material Fig. S4A). We then followed the dynamics of GFP::PEEL-1 during the first embryonic divisions and observed similar overall dynamics governed by the MTOC displacement as for the sperm mitochondria, suggesting that the MTOC-driven dynamics is an autophagosome characteristic rather than a substrate-specific property (Fig. 2B and supplementary material Movie 2). To reinforce this conclusion, we observed the dynamics of GFP::LGG-2 and revealed the same preferential pericentrosomal localization during the first embryonic division (88%, n=9) (supplementary material Movie 3). In order to visualize the connection with the microtubules emanating from the MTOC we visualized simultaneously the sperm mitochondria, the microtubules and the nuclear DNA in fixed wild-type embryos and observed sperm mitochondria aligned along astral microtubules during the first mitosis (n=11) (Fig. 2C). Together, our data suggest that sperm mitochondria in allophagosomes tend to concentrate around mitotic MTOC in the one-cell-stage *C. elegans* embryo.

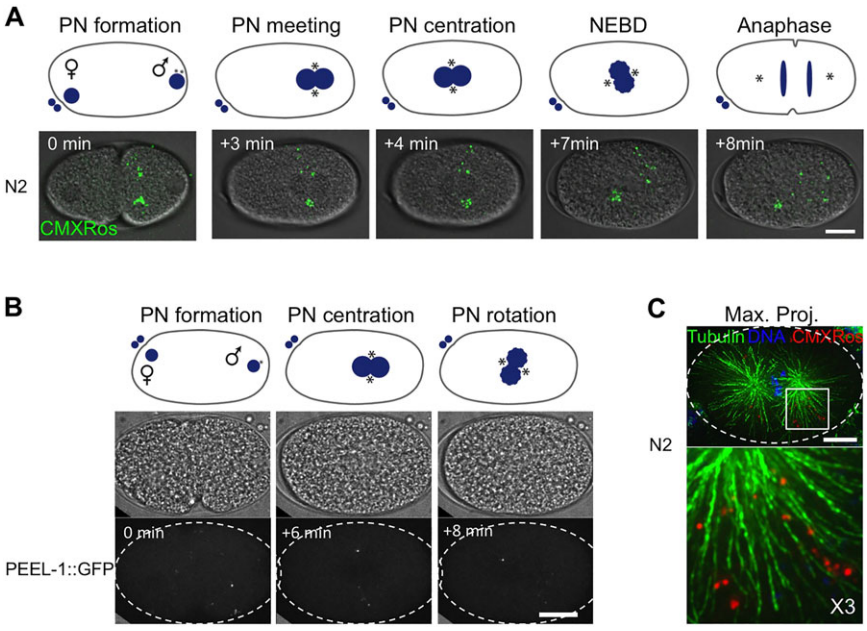

Fig. 2. The spatial distribution of allophagy substrates depends on MTOC and microtubule dynamics during the first embryonic divisions. (A) Schematic representation of the first mitosis of a wild-type embryo (upper panel), MIP and DIC from a time-lapse recording showing the dynamics of sperm mitochondria (green) at indicated stages (supplementary material Movie 1). (B) Schematic representation, transmission and MIP from time-lapse recording of an embryo fertilized by a spermatozoid expressing PEEL-1::GFP, at pronuclei (PN) formation, PN centration and PN rotation stages. MOs tend to cluster around the centrosomes and follow the pronuclei/centrosome complex during its centration prior the first zygotic division. (C) MIP of deconvolved immunofluorescence images showing sperm mitochondria (red), DNA (blue) and α-tubulin (green) in a wild-type embryo (N2) (top panel), and a threefold magnified view of the highlighted area around the MTOC (bottom panel). Scale bars: 10 µm.

Development (2015) 142, 1705-1716 doi:10.1242/dev.117879

LGG-2 is required for the microtubule-dependent allophagosome dynamics during the first embryonic divisions

In order to characterize the LGG-2 function in the distribution of allophagosomes and their substrates, we followed sperm-mitochondria dynamics in embryos expressing β-tubulin and histone fused to GFP in wild-type and *lgg-2(tm5755)* backgrounds (100%, *n*=6) (Fig. 3A). We confirmed that sperm-inherited mitochondria tend to follow mitotic centrosomes in the wild-type background, whereas the clustered mitochondria in the *lgg-2(tm5755)* background remained at the anterior cell cortex and uncoupled from the movement of the centrosomes/pronuclei complex during its centration (87.5%, *n*=8) (Fig. 3A and supplementary material Movie 4). This clustering phenotype depends on the entry into autophagosomes, as sperm-inherited mitochondria were scattered in LGG-1 RNAi depletion in both wild-type and *lgg-2(tm5755)* backgrounds (supplementary material Movie 5).

To confirm that sperm-inherited mitochondria dynamics is dependent on microtubules, we depolymerized the microtubules using nocodazole, and tested the impact on the dynamics of the sperm-inherited mitochondria in the strain expressing β-tubulin and histone fused to GFP in a wild-type background (Fig. 3B). In presence of nocodazole, microtubules were depolymerized, and sperm-inherited mitochondria remained mostly clustered at the cell cortex. This phenotype, similar to the clustering observed in *lgg-2 (tm5755)*, was not due to a defect in LGG-2 recruitment, as we detected a normal LGG-2 signal around the clustered MO (Fig. 3C).

Sperm-inherited mitochondria movement toward the centrosomes suggested that a minus end-directed motor could play a role. We therefore tested whether the RNAi depletion of the dynein heavy chain subunit (DHC-1) would affect this retrograde transport of the substrates and allophagosomes. As expected, DHC-1 RNAi depletion induces multiple defects at the one-cell stage, including meiosis and centrosome separation defects, the lack of pronuclei migration and their asynchronous nuclear envelope breakdown (Gönczy et al., 1999). We monitored the dynamics of sperm-inherited mitochondria in RNAi-treated embryos. Using DIC microscopy, we observed pronuclei migration defects and asynchronous breakdown in 66% of the embryos (*n*=9), but the reliable tracking of the centrosomes was difficult and made our conclusions uncertain concerning the uncoupling of sperm-inherited mitochondria migration toward centrosomes. We therefore conducted the DHC-1 RNAi depletion in embryos expressing GFP::TBG-1 to visualize pericentrosomal material. In 100% of the embryos recorded from the time of male PN envelope breakdown (*n*=5), we did not observe retrograde movements of sperm-inherited mitochondria during the first embryonic mitosis (Fig. 4A and supplementary material Movie 6), and the distal distribution of sperm mitochondria from centrosomes was confirmed in all fixed one-cell-stage embryos (*n*=9) (Fig. 4B). Although in all embryos observed at this stage (*n*=14), the sperm mitochondria tended to remain away from the centrosomes, and they were not clustered as observed in *lgg-2(tm5755)* mutants (Fig. 4A,B and supplementary material Movie 6). In order to confirm that the impact of DHC-1 RNAi depletion on preventing sperm mitochondria gathering around centrosomes was representative of allophagosome dynamics rather than a problem in their formation, we monitored allophagosome dynamics in embryos expressing GFP::LGG-1. Remarkably, in 71% (*n*=7) of the DHC-1 RNAi-treated embryos, allophagomes were strongly clustered, as normally observed in *lgg-2(tm5755)* mutant embryos (Fig. 4C and supplementary material Movie 7). Indeed, we observed that the overexpression of GFP::LGG-1 in wild-type animals is correlated with a clear reduction of LGG-2 signal in 100% of the one-cell-stage embryos observed (*n*=15 for GFP::LGG-1 and *n*=24 for N2), even in the area of the clustered allophagosomes (Fig. 4D). We therefore concluded that GFP::LGG-1 expression leads to the reduction of LGG-2 protein in allophagosomes and to the phenotype associated with the loss of LGG-2 from allophagosomes.

We next tested whether the lack of retrograde transport observed in the *lgg-2(tm5755)* embryos could be the consequence of allophagosome clustering. Unlike described previously (Manil-Ségalen et al., 2014), we observed that the expression of GFP::LGG-1 in the germ line promotes the clustering of allophagosomes in 78% of the embryos recorded from PN to the two-cell stage (*n*=14) (Fig. 4D and supplementary material Movie 8). The clustering appeared stronger and slightly more frequent when the strain was grown at 24°C rather than 16°C (6 out of 7 and of 5 out of 7, respectively). The stronger phenotype observed at 24°C was correlated with a 3.5-fold increase of GFP::LGG-1 expression

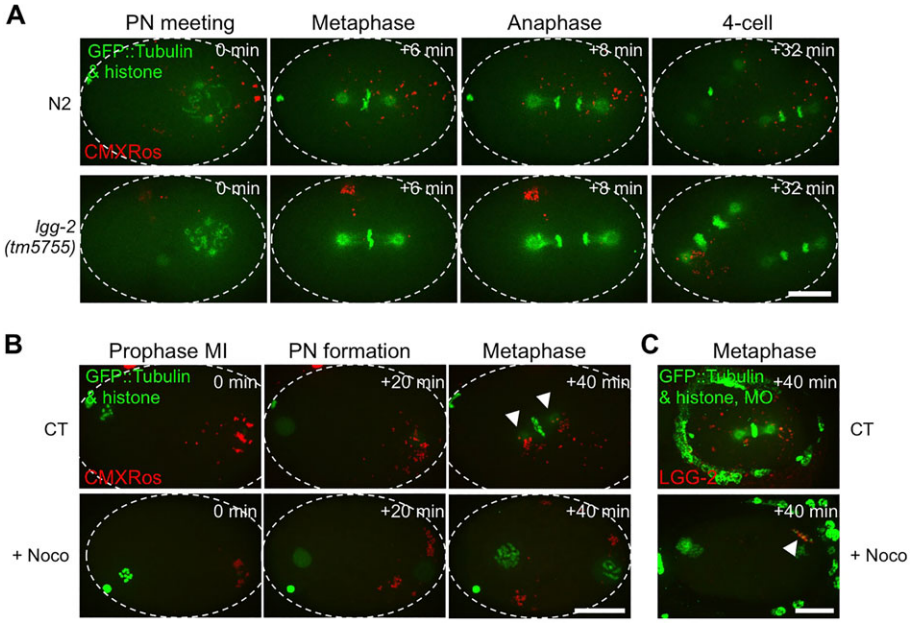

Fig. 3. LGG-2 is required for the microtubule-dependent allophagosome dynamics during the first embryonic divisions. (A) MIP from time-lapse recordings of wild-type and *lgg-2(tm5755)* embryos expressing GFP::β-tubulin and GFP::histone (green), showing the distribution of sperm mitochondria (red) at indicated stages (supplementary material Movie 4). (B) MIP from time-lapse recordings of control (CT) and nocodazole-treated (+Noco) embryos expressing GFP::β-tubulin and GFP::histone (green), showing the distribution of mitotracker-labeled sperm mitochondria (red). Centrosomes are highlighted (arrowheads). (C) MIP of confocal images of control (CT) and nocodazole-treated (+Noco) embryos expressing GFP::β-tubulin; GFP::histone (green) and stained for MO (green) and LGG-2 (red). LGG-2^{+} MOs are highlighted (arrowhead). Scale bars: 10 µm.

Development (2015) 142, 1705-1716 doi:10.1242/dev.117879

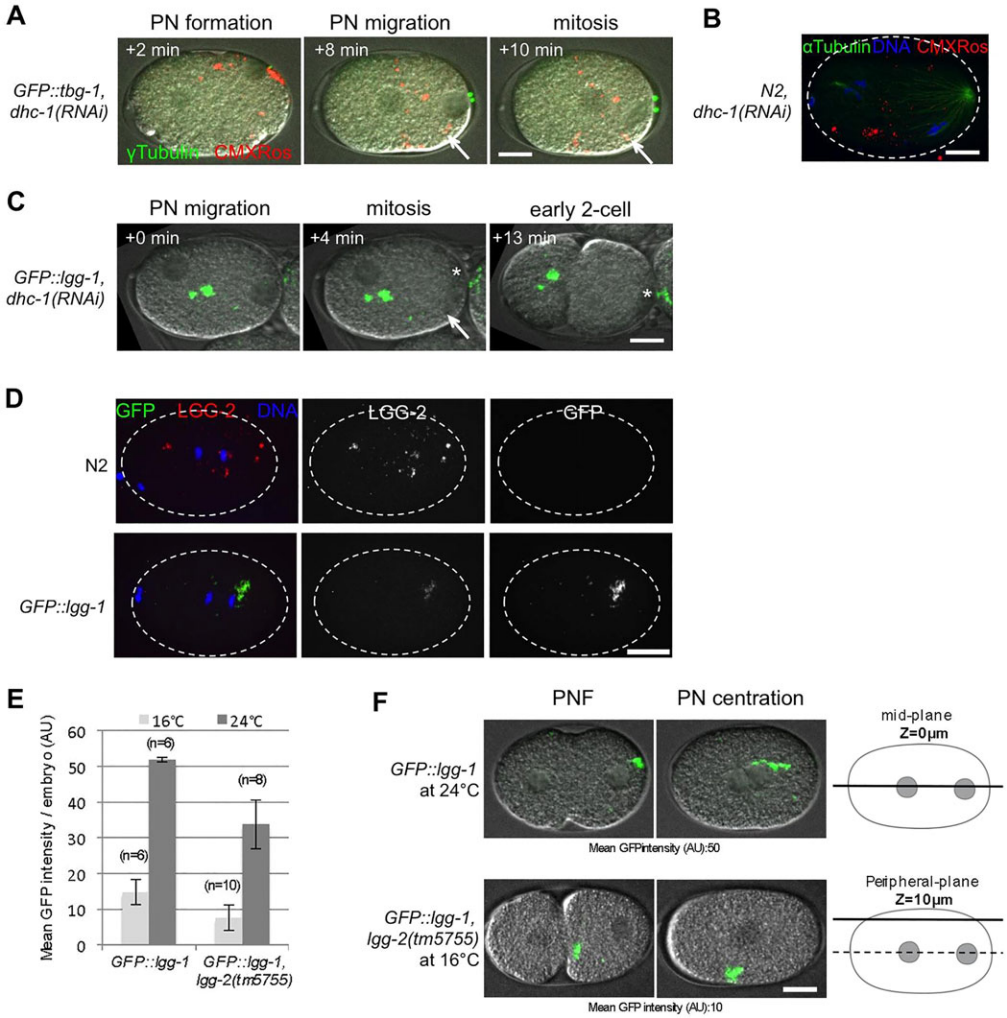

Fig. 4. LGG-2 is required for retrograde transport of allophagosomes. (A) MIP and DIC from time-lapse recordings of a *dhc-1 (RNAi)* embryo expressing GFP::γ-tubulin (green) and sperm mitochondria (red) (supplementary material Movie 6). (B) MIP confocal image of a *dhc-1(RNAi)* embryo and sperm mitochondria (red) stained for α-tubulin (green) and DNA (blue). Sperm mitochondria moving away from the centrosomes are highlighted (arrows). (C) MIP and DIC from time-lapse recordings of a *dhc-1(RNAi)* embryo expressing GFP::LGG-1 (green) (supplementary material Movie 7). Sperm mitochondria are clustered away from the highlighted mitotic bundle of microtubules (arrow). (D) MIP confocal images of N2 and GFP::LGG-1 (green) embryos stained for LGG-2 (red) and DNA (blue). (E) Quantitative analysis of GFP::LGG-1 intensity at 16°C and 24°C of wild-type and *lgg-2(tm5755)* embryos expressing GFP::LGG-1. (F) Single GFP and DIC planes from time-lapse recordings of wild-type (top panels) and *lgg-2(tm5755)* (bottom panels) embryos expressing GFP::LGG-1 (green) (supplementary material Movie 8). Scale bars: 10 μm.

level at 24°C compared with 16°C (Fig. 4E). The mean GFP intensity per embryo was 52±0.7 arbitrary units (AUs) at 24°C compared with 15±3.5 AUs at 16°C (n=6 for each) (Fig. 4E). Interestingly, in 85% of the embryos recorded (n=14), the clustered allophagosomes tend to follow the centrosome migration during centration and rotation. Alternatively, in 100% of *lgg-2 (tm5755)* embryos expressing GFP::LGG-1 (n=18), the clustered allophagosomes were at the cell cortex and did not follow the centrosomes while they migrate and rotate (Fig. 4F and supplementary material Movie 8). The lack of retrograde transport was therefore correlated with the reduction of LGG-2 (Fig. 4D), suggesting that GFP::LGG-1 overexpression itself is sufficient to trigger the clustering of allophagosomes but is not responsible for the lack of retrograde transport.

Altogether, our results demonstrate that the absence of LGG-2 prevents the dynein-dependent retrograde transport of LGG-1$^+$ allophagosomes toward the pericentrosomal area, suggesting that LGG-2 is recruited in the allophagosome membranes to mediate their microtubule-driven gathering around mitotic centrosomes.

LGG-2 is essential for allophagosome motility on microtubules to gain the lysosome-rich pericentrosomal area

The abnormal cortical clustering of allophagosomes in the *lgg-2* mutant was correlated with a delay in substrate clearance, suggesting that the absence of LGG-2 might interfere with autophagosome maturation and fusion with acidic compartments. We therefore observed the dynamics of the lysosomes in *C. elegans* embryos using lysotracker to label intracellular acidic compartments. The lysotracker-labeled structures accumulated around the two centrosomes by the stage of pronuclei meeting and follow the displacement of the centrosomes/pronuclei complex during their centration and rotation. The maximum of pericentrosomal enrichment was achieved by metaphase of the first mitosis (100%, n=7) (Fig. 5A and supplementary material Movie 9). To confirm that lysotracker-positive structures enriched around the centrosomes correspond to lysosomes we labeled the endogenous homolog of the lysosome-associated membrane protein 1 (LMP-1) (Kostich et al., 2000) on fixed embryos (supplementary material Fig. S4C,D and supplementary material Movie 11). We also observed mCherry-tagged NUC-1, a lysosomal nuclease involved in the degradation of apoptotic cell DNA (Wu et al., 2000) in living embryos (supplementary material Fig. S4B). Both lysosomal markers accumulated around the two centrosomes by the stage of pronuclei meeting and followed the displacement of the centrosomes/pronuclei complex during its centration and rotation (100%, n=2) (supplementary material Fig. S4B,C and supplementary material Movies 10 and 11). We therefore considered that lysotracker-positive structures gathered around the centrosomes during mitosis correspond to acidic lysosomal compartments. In wild-type embryos, we could observe

Development (2015) 142, 1705-1716 doi:10.1242/dev.117879

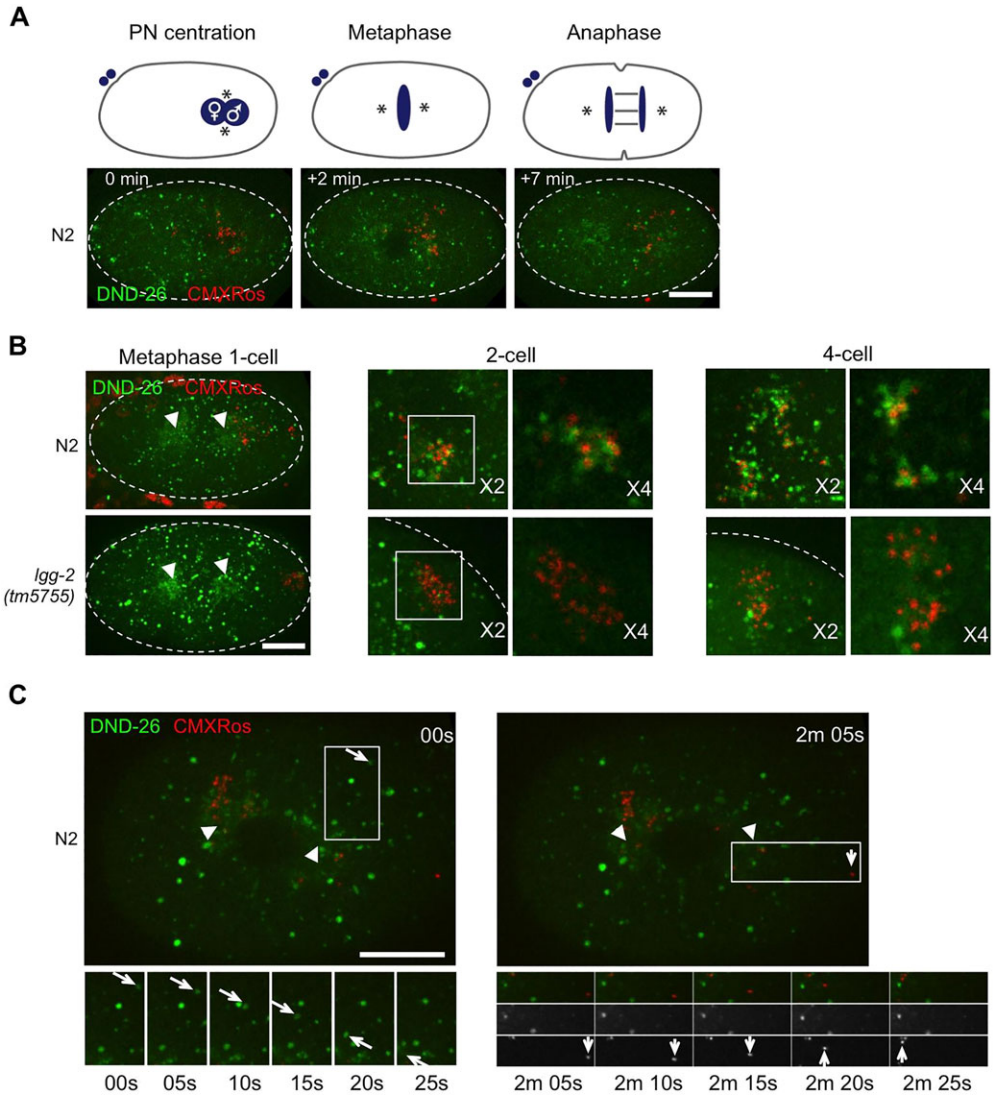

Fig. 5. Sperm-inherited mitochondria remain distant from pericentrosomal acidic compartments in the absence of LGG-2. (A) Schematic representation and single planes from time-lapse recordings of wild-type (N2) embryos showing acidic compartments (green) and sperm mitochondria (red) (supplementary material Movie 9). (B) MIP or single plane from time-lapse recordings of wild-type (N2, top panels) and *lgg-2(tm5755)* (bottom panels) embryos showing acidic compartments (green) and sperm mitochondria (red) (supplementary material Movie 12). Twofold (MIP) and fourfold (single plane) magnified views of the highlighted areas containing sperm mitochondria in pericentrosomal (for the N2) and cortical [for the *lgg-2(tm5755)*] regions. (C) MIP from time-lapse recordings of a wild-type (N2) embryo at pronuclei rotation stage showing acidic compartments (green) and sperm mitochondria (red) motility toward the centrosomes (arrowheads), and consecutive images (below) showing the rapid movement of a DND-26^{+} vesicle (arrows in the left panels) and a sperm mitochondrion (arrows in the right panels) (supplementary material Movie 13). The moving sperm mitochondria do not colocalize with DND-26 signal. Scale bars: 10 µm.

the co-gathering of acidic compartments and sperm-inherited mitochondria around the centrosomes starting as early as during the first mitosis, suggesting that acidification is occurring (Fig. 5B and supplementary material Movie 12).

We then tested whether the alteration in the dynamics of the allophagosomes and their substrates is correlated with a defect in their acidification. We monitored *lgg-2(tm5755)* embryos colabeled for sperm mitochondria and the lysosomes. Importantly, in the absence of LGG-2, the distribution of the lysosomes was identical to the wild-type embryos, thus demonstrating that LGG-2 is not required for pericentrosomal enrichment of the lysosomes (Fig. 5B; supplementary material Fig. S4B,C and supplementary material Movies 10 and 11). In the *lgg-2(tm5755)* embryos, the cortical cluster of sperm mitochondria remained away from the pericentrosomal lysosome-rich region (82%, n=11) (Fig. 5B and supplementary material Movie 12); eventually, rare colocalization events occurred from the four-cell stage in *lgg-2(tm5755)* mutants (90%, n=33) (Fig. 5B and supplementary material Fig. S4D). The defect in pericentrosomal re-localization during mitosis and the absence of co-staining with the lysosomal marker suggested that the defect in allophagosome acidification could be the consequence of a defect in their migration. In order to establish the sequence of events leading to the acidification of autophagosomes, single lysosomes and mitochondria were tracked. We observed movements of lysosomes and of 24 sperm mitochondria toward the centrosomes (Fig. 5C and supplementary material Movie 13). Seventy-one percent of the mitochondria moved for two or more consecutive images, following linear trajectories. Their average speed was 0.64±0.18 µm/s (s.d.) for an average covered distance of 8±2.9 µm (s.d.) Importantly, for all moving 24 mitochondria, the retrograde movement occurred without colocalization with the lysotracker (Fig. 5C and supplementary material Movie 13), demonstrating that acidification is not a prerequisite to sperm mitochondria pericentrosomal directed movement.

LGG-2 is essential for RAB-7^{+} allophagosome transport to the pericentrosomal area

In order to identify the defective step in allophagosome maturation and acidification in the absence of LGG-2 we localized the small GTPases Ce-Rab5 (RAB-5) and Ce-Rab7 (RAB-7) that regulate membrane traffic into and between early-to-late endosomes. During the early steps of endocytosis, Rab5 regulates the transport of clathrin-coated vesicles from the plasma membrane to the early endosome, the homotypic early endosomes fusion (Bucci et al., 1992; Gorvel et al., 1991) and their attachment to microtubules (Nielsen et al., 1999). Rab5^{+} early endosomes and their cargos

Development (2015) 142, 1705-1716 doi:10.1242/dev.117879

concentrate in progressively larger but fewer endosomes that migrate from the cell periphery to the perinuclear area where the exchange of Rab5 for Rab7 occurs (Rink et al., 2005). We localized endogenous RAB-7 in the wild-type and *lgg-2(tm5755)* fixed embryos together with labeled sperm organelles. Whereas, very few of the sperm-inherited mitochondria and MO were associated with RAB-7 signal during meiosis II in wild-type embryos (Fig. 6A and data not shown), after metaphase, a significant fraction of the pericentrosomal sperm mitochondria were surrounded by RAB-7 signal (Fig. 6A). In all *lgg-2(tm5755)* embryos, despite the loss of pericentrosomal localization of the substrates, RAB-7 signal was enriched around the clustered MO (n=42) (Fig. 6C and supplementary material Movie 14) and sperm mitochondria (n=47) (Fig. 6A and supplementary material Movie 14), as shown in the

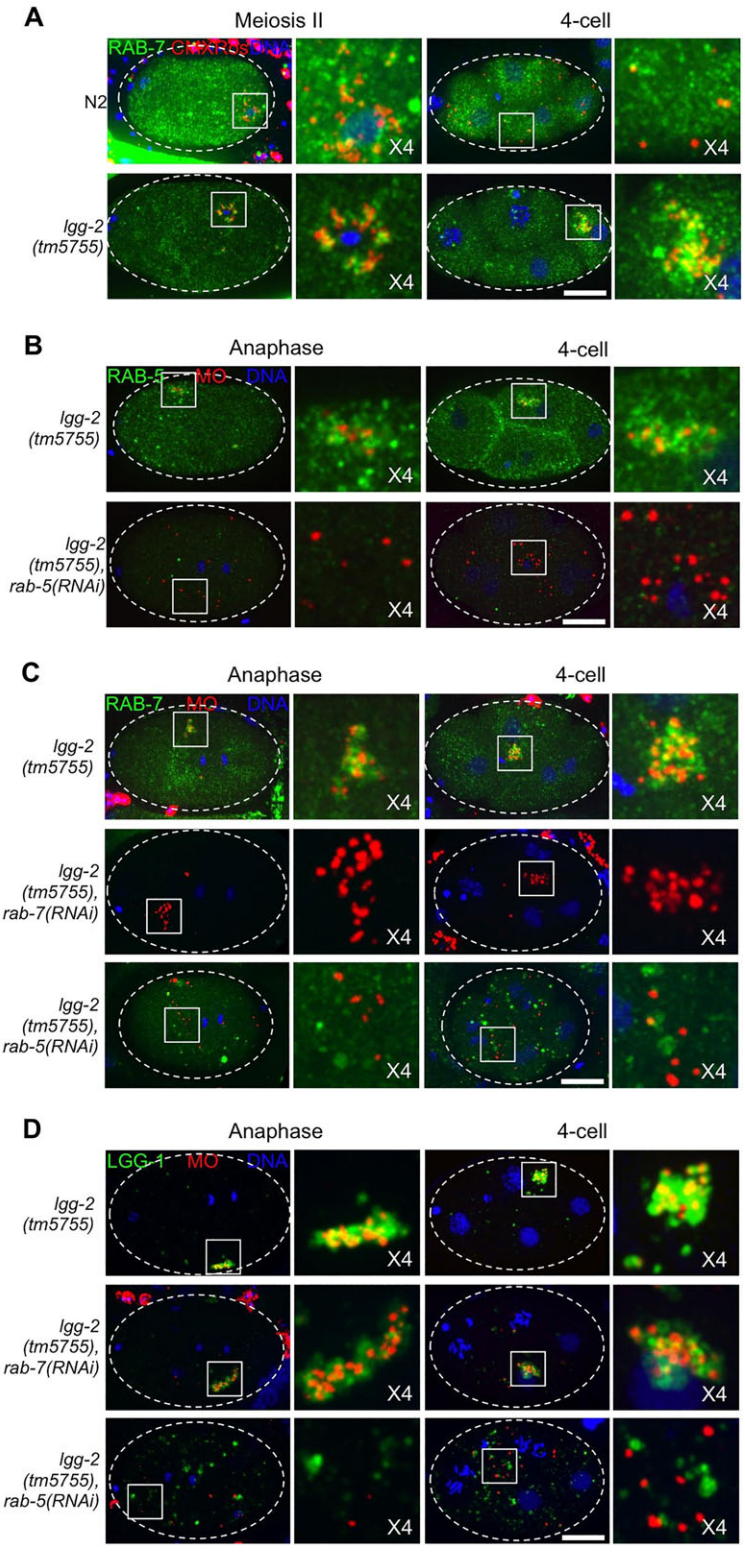

Fig. 6. RAB-5 is required for allophagosome formation and LGG-2 is required for their maturation downstream of RAB-7. (A) MIP of confocal images of wild-type (N2, top panels) and *lgg-2(tm5755)* embryos (bottom panels) stained for RAB-7 (green), sperm mitochondria (red) and DNA (blue). (B) Single-plane images of *lgg-2 (tm5755)* and *lgg-2(tm5755);rab-5(RNAi)* embryos stained for RAB-5 (green), MO (red) and DNA (blue). (C) MIP confocal images of *lgg-2 (tm5755)*, *lgg-2(tm5755);rab-7(RNAi)* and *lgg-2(tm5755);rab-5(RNAi)* embryos stained for RAB-7 (green), MO (red) and DNA (blue). (D) MIP confocal images of *lgg-2(tm5755)*, *lgg-2(tm5755);rab-7(RNAi)* and *lgg-2(tm5755);rab-5(RNAi)* embryos stained for LGG-1 (green), MO (red) and DNA (blue), and fourfold magnified views of the highlighted areas. Scale bars: 10 µm.

Development (2015) 142, 1705-1716 doi:10.1242/dev.117879

four-cell-stage embryos. This signal was specific for RAB-7, as the signal was absent from *rab-7(RNAi)* embryos (Fig. 6C). The observation that, in the absence of LGG-2, allophagosomes were arrested in a RAB-7$^+$ stage indicates that LGG-2 is required for the centripetal movement of RAB-7$^+$ but non-acidic allophagosomes.

Interestingly, the clustered substrates in the absence of LGG-2 were also associated with RAB-5 signal (72%, *n*=36) (Fig. 6B), suggesting that the RAB-5 GTPase participates in allophagosome formation and/or maturation. To confirm this hypothesis we tested the impact of RAB-5 RNAi depletion on the distribution of the MO and on the formation of the allophagosomes in the early *lgg-2 (tm5755)* embryos. Upon RNAi depletion, RAB-5 signal was strongly reduced (Fig. 6B), and the substrates were no longer clustered (100%, *n*=78) nor associated with LGG-1 signal (85%, *n*=26) (Fig. 6D), demonstrating that RAB-5 is required for allophagosome formation prior LGG-2 function.

Together, these results show that LGG-2 function is downstream of RAB-5 and RAB-7 roles in allophagosome maturation and is essentially involved in their centripetal migration, a step preceding, and probably facilitating, their fusion with the pericentrosomal acidic lysosomal compartments.

DISCUSSION

The role of Ce-LC3/LGG-2 in autophagy has been previously studied in the *lgg-2(tm5755)* embryos and led the authors to propose that LGG-2 is required for allophagosomes acidification, a function that would be mediated by an interaction with VPS-39, a component of the HOPS complex (Manil-Ségalen et al., 2014). In the absence of LGG-2 protein, LGG-1 was still recruited around the substrates that appeared clustered in the early embryos. This striking clustering phenotype of the allophagosomes was attributed to an acidification defect (Manil-Ségalen et al., 2014). In this previous study, the impact on the substrates clearance and how preventing acidification could trigger the persistence of the clustered allophagosomes was not addressed. In our study, we show how the absence of detectable full length LGG-2 impacts on the efficiency of the degradation of sperm-inherited organelles and how it induces the persistence of the clustered allophagosomes.

Importantly, as the overexpression of LC3 protein is prone to induce aggregation and defect in autophagy (Klionsky et al., 2012; Politi et al., 2014), we analysed a second *lgg-2* mutant [*lgg-2(tm6474)*] and observed the same phenotype of allophagosome clustering, despite the fact that it would produce, if any, a very different polypeptide, sharing only 23 amino acids (aa) [compared with 80 aa for the *lgg-2(tm5755)* allele] with the N-terminal sequence of LGG-2 and lacking the ubiquitin-like domain and the C-terminal glycine residue required for membrane anchoring. Altogether, it demonstrates that both *lgg-2 (tm5755)* and *lgg-2(tm6474)* mutants must be considered as loss-of-function mutants, implying that the clustering phenotype is due to the absence of LGG-2. Importantly, the absence of full-length LGG-2 did not prevent the recruitment of LGG-1 around sperm-inherited organelles, allowing the analysis of LGG-2-specific functions. We measured the stability of MO and sperm mitochondria in wild-type versus *lgg-2(tm5755)* embryos and detected a transient stabilization of both structures, with 4-5 times more remaining signal in the mutant embryos. In later developmental stages, we did not detect any substrates left, showing that the absence of LGG-2 is slowing down the degradation process rather than blocking it. This conclusion was strengthened by the comparison with the *lgg-1* mutation that had a much more severe effect on the degradation, as MO and sperm mitochondria were still detected in the dead L1 larvae (Al Rawi et al., 2011; Sato and Sato, 2011).

Interestingly, the stabilizing effect on substrates observed in the absence of full-length LGG-2 in both *lgg-2* mutants was correlated with the radical modification of the substrate distribution within and between the blastomeres. The substrates, in LGG-1$^+$ allophagosomes, remained clustered and at the periphery of the cell. Actually, a similar clustering of the substrates is observed upon fertilization, when the spermatozoid fuses with the large oocyte, bringing together its nuclear DNA, surrounded by mitochondria and MO. In wild-type embryos, this remained visible during the first 30 min and tended to move with the maternal mitochondria and yolk toward the anterior pole of the one-cell-stage embryo at the time of the contraction of the cortical acto-myosin cytoskeleton (Munro et al., 2004; Strome, 1986). During pronuclei migration, sperm-inherited organelles in allophagosomes tended to move toward the mitotic centrosomes and to follow the centration and rotation of the centrosomes/pronuclei complex. This pericentrosomal gathering was maximal during the anaphase of the first mitotic division. The localization of the sperm mitochondria along the astral microtubules and the importance of DHC-1 strengthened the conclusion that allophagosomes were transported along microtubules. As a result, the residual substrates within allophagosomes were scattered within and between AB and P1 blastomeres. In the absence of LGG-2, allophagosomes remained clustered at the cell cortex and uncoupled from the movement of the centrosome/pronuclei complex until the four-cell stage, showing that allophagosomes failed to connect and move along the microtubules. This uncoupling leads to the transmission of all allophagosomes to a single blastomere, reducing the dilution of the substrates.

The persistent cortical clustering phenotype seen in the two- to four-cell stage of *lgg-2* mutant embryos requires the entry of the substrates in LGG-1$^+$ allophagosomes. Once allophagosomes were formed, the cluster of substrates persisted in the absence of LGG-2 or upon microtubules depolymerization. Altogether, this demonstrates that the clustering phenotype was not a default property of the substrates when not engaged in the autophagy pathway, but the consequence of a defective step in the autophagy pathway that required LGG-2 and microtubules. This conclusion differs from the one reached in work on mice and the proposed passive model of paternal mitochondria distribution after fertilization (Luo et al., 2013a). Based on our observation, we propose that LGG-2, the counterpart of LC3 in the worm, is required for the microtubule-dependent dynamics of the autophagosomes in charge of sperm mitochondria degradation. Another striking result was that a modest germline overexpression of GFP::LGG-1 also promotes the persistence of the allophagosome cluster. This side effect of germline expression of GFP::LGG-1 has been largely ignored and underestimated before, even though it could be inferred from previously published data (Manil-Ségalen et al., 2014). Our analysis revealed that GFP-LGG-1-promoted clustering was more transient than that observed in the absence of LGG-2. Furthermore, the clustered substrates were still able to follow centrosome movement during centration and rotation in an LGG-2-dependent manner. This demonstrates that the clustering per se is not responsible for the absence of retrograde movement of allophagosomes observed in the *lgg-2(tm5755)* mutant. Interestingly, we observed a reduction of LGG-2 signal in the clustered GFP::LGG-1 allophagosomes, suggesting that GFP::LGG-1 interferes with the recruitment of LGG-2, supporting the conclusion that LGG-2 recruitment is an important step to allow retrograde movement of allophagosomes. This observation using GFP::LGG-1 reveals the limitations of this marker to study autophagy flux, as it interferes with the process.

Development (2015) 142, 1705-1716 doi:10.1242/dev.117879

Autophagosome dynamics along microtubules has been observed in ganglion neurons, where autophagosomes containing mitochondria displayed dynein-driven movement toward the MTOC in the cell soma, thus allowing their gradual acidification (Maday et al., 2012). The altered dynamic in the *lgg-2(tm5755)* mutant was therefore potentially responsible for a defect in allophagosome maturation and could explain the transient stabilization of the sperm-inherited components. This hypothesis was validated by several observations. First, we demonstrated that LGG-1^{+} allophagosomes clustered at the cell periphery remained mostly negative for the fluorescent lysosomal marker, suggesting that the absence of LGG-2 prevented their migration early in their maturation process. The second strong argument was that, in wild-type embryos, sperm mitochondria showing retrograde movements were not associated with lysotracker, demonstrating that migration occurred prior to acidification.

Here, we demonstrated that the small GTPases regulating membrane trafficking were retained in the allophagosome clusters observed in the absence of LGG-2. This implied that LGG-2 is acting on allophagosomes positive for RAB-5 and RAB-7. Furthermore, we demonstrated that RAB-5, but not RAB-7, is required for allophagosome formation. Our observations provide evidences for a role of Rab-5 and Rab-7 GTPases and an endosomal origin for the allophagophore formation. Indeed, the Rab machinery could be common to several vesicular trafficking pathways involving LC3 proteins, including phagocytosis and entosis (Li et al., 2012). Morphological studies showed that the endocytosis and the autophagy pathways are able to converge to form amphisomes that are prelysosomal chimeric vesicles (reviewed by Eskelinen et al., 2011). Amphisomes were also described in *C. elegans* embryos, where VPS-27^{+} endosomes and allophagosomes were proposed to fuse in an LGG-2 independent manner (Manil-Ségalen et al., 2014). In *Drosophila* as well, paternal mitochondria were eliminated by a new mechanism related to endocytosis and autophagy (Politi et al., 2014). During this process, endosomal and autophagy markers were colocalized but Rab5 was not visualized, possibly due to a rapid exchange of Rab5/Rab7 (Politi et al., 2014). Similarly, we did not see massive colocalization between RAB-5 and RAB-7 and the allophagy substrates in wild-type *C. elegans* embryos. However, our observations that allophagosomes remained RAB-7^{+} in the absence of LGG-2 support the idea that the displacement was a prerequisite for complete acidification and that the defect associated with the absence of LGG-2 was primarily due to a defect in the motion (see model in Fig. 7) rather than in the acidification itself as proposed before (Manil-Ségalen et al., 2014). Along this line, the lack of retrograde transport in the absence of LGG-2 was correlated with a delay in the clearance of allophagy substrates, consistent with a delay in allophagosome acidification due to a locomotion defect rather than a total impediment of acidification. Indeed, even in the absence of LGG-2, we observed rare colocalization events between the substrates and the lysotracker in the cluster region of early embryos or, more frequently, at later developmental stages, and the substrates were eventually cleared. This suggests that allophagosomes and acidic lysosomal compartments are able to fuse when they meet by chance, a probability that might be increased with the reduction of the cell volume as a consequence of the consecutive zygotic cell divisions. Finally, another observation that we interpret as reinforcing our conclusion that the complete maturation and acidification is not a prerequisite to the autophagosomes migration comes from the observations that, in *vps-39* and *vps-41* mutants, autophagosomes were localized in the perinuclear region (Manil-Ségalen et al., 2014), a localization that we interpret and visualized (data not shown) as pericentrosomal.

Our observations made in *C. elegans* embryos on the function of LGG-2/LC3 in targeting allophagosomes to the pericentrosomal region to increase their probability to meet and fuse with the lysosomes are consistent with earlier observations that autophagosomes in mammalian cells are preferentially formed in the peripheral zone of the cytoplasm, then delivered to the vicinity

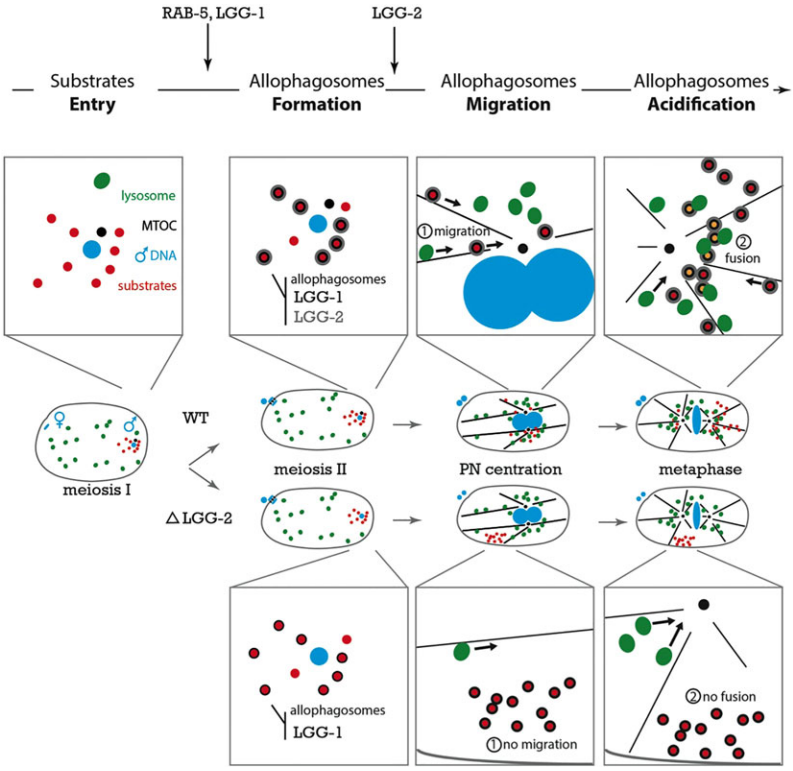

Fig. 7. Model for the function of Ce-LC3/LGG-2 in the migration of allophagosomes toward the MTOC prior to their acidification. At meiosis I, sperm mitochondria and MO are grouped around sperm DNA. During meiosis II, LGG-1^{+} autophagosomes are formed around sperm-inherited organelles (allophagy substrates) and require the GTPase RAB-5. In wild-type embryos, LGG-2 is recruited to the allophagosomes and allows their migration along microtubules toward the pericentrosomal area during the first mitosis, favoring their meeting and fusion with acidic compartments. In the absence of LGG-2, the LGG-1^{+} autophagosomes remain clustered in a cortical region of the one-cell-stage embryo, reducing their probability to meet and fuse with the pericentrosomal acidic compartments, thus delaying the clearance of the substrates.

Development (2015) 142, 1705-1716 doi:10.1242/dev.117879

of the lysosomes near the MTOC in a dynein/microtubule-dependent manner (Jahreiss et al., 2008). The Dynein knockdown decreased the fusion of autophagosomes with lysosomes, stabilized the autophagic substrate α-synuclein and blocked the autophagic flux (Jahreiss et al., 2008; Ravikumar et al., 2005). In addition, in cells overexpressing GFP-LC3, the autophagosomes were preferentially localized around the MTOC (Jahreiss et al., 2008). Our conclusion that LGG-2/LC3 is involved in the retrograde transport of early allophagosomes is consistent with LC3 having been identified as an abundant neuronal light chain of the microtubule-associated proteins 1A and 1B (Kuznetsov and Gelfand, 1987; Mann and Hammarback, 1994). Interestingly, LC3 binds directly to microtubules *in vitro* (Kouno et al., 2005; Mann and Hammarback, 1994); thus, LGG-2 might link directly allophagosomes to microtubules but, as we could not reveal such physical interaction in worms, we cannot exclude the existence of intermediate molecules bridging LGG-2 to microtubules.

It would be interesting to test whether this function of LGG-2/LC3 in the control of allophagosome dynamics discovered in *C. elegans* embryos is conserved in other species in which autophagy markers are localized around sperm-inherited mitochondria (Al Rawi et al., 2011; Luo et al., 2013a; Politi et al., 2014), and how crucial this LC3 function would be in the efficiency of their degradation and in the segregation of the mitochondria between early blastomeres.

MATERIALS AND METHODS

C. elegans strains and RNAi

Nematode strains were grown and handled as described (Brenner, 1974). Strains carrying the mutations *lgg-2(tm5755)*, *lgg-2(tm6474)* and *atg-3 (bp412)* were used. The *lgg-2(tm5755)* mutant was backcrossed to wild-type twice prior to our analyses. *lgg-2(tm5755)* and *lgg-2(tm6474)* mutations were tracked by PCR genotyping using the primers shown in the supplementary material methods. The quantitative RT-PCR analysis was performed on total RNA extracts of N2, *lgg-2(tm6474)* and *lgg-2(tm5755)* using the primers listed in supplementary material Table S1.

Transgenic strains used in this study are described in the supplementary material methods. Bacterial clones from the J. Ahringer library (*atg-7*, *dhc-1*, *lgg-1*, *rab-5*, *rab-7* and empty vector L4440 for control) were used for RNAi as previously described (Al Rawi et al., 2011), except for *atg-5 (RNAi)*, which was carried out for two generations.

Immunofluorescence staining and antibodies

C. elegans embryo immunostaining was performed as previously described (Galy et al., 2003), except for LMP-1 (Miller and Shakes, 1995) with the modifications described in the supplementary material methods. The primary and secondary antibodies used are listed in supplementary material Table S2.

Lysotracker/mitotracker staining and nocodazole treatment

Sperm mitochondria labeling with CMXRos (Invitrogen) was performed as previously described (Al Rawi et al., 2011). Gravid hermaphrodites were dissected in meiosis medium (Askjaer et al., 2014) containing 0.5 µM lysotracker (DND-26, Invitrogen) to label acidic compartments or 0.8 µM nocodazole (Sigma-Aldrich) to depolymerize microtubules, and were mounted for live imaging. To test the effect of the nocodazole treatment on the recruitment of LGG-2 around the MO, embryos were incubated with nocodazole for 40 min prior to fixation.

Fluorescence imaging

The live imaging of the embryos mounted in meiosis buffer on agarose pads was performed as described (Askjaer et al., 2014) on a spinning-disk confocal microscope (Roper Scientific). Time-lapse images were acquired at 1-min intervals (except when specified). The imaging of fixed embryos was carried out as *z*-stacks of images on the same spinning-disk confocal microscope except for Fig. 3C (see supplementary material methods for details).

The quantitation of the fluorescence intensity of MO, sperm mitochondria as well as GFP::LGG-1 signal was performed on *z*-stacks of images acquired on a spinning-disk confocal microscope. The acquisitions and quantifications were performed as described in the supplementary material methods.

TEM

TEM analysis was performed as previously described (Al Rawi et al., 2011), with the modifications described in the supplementary material methods.

Acknowledgements

We are very grateful to O. Renaud from the Institut Curie for giving us access and advice on the Deltavision Core deconvolution microscope; to the staff of the IBPS imaging platform for their efficient help with DIC spinning disk imaging; to T. Le, E. M. Daldello, V. Peletier and R. Zamy for valuable technical assistance during all stages of this project and to K. Wassmann for shared group meetings and valuable discussions. We are also very grateful to H. Zhang (State Key Laboratory of Biomacromolecules, Institute of Biophysics, Chinese Academy of Sciences, Beijing, China), S. Strome (Department of MCD Biology, Sinsheimer Labs, UCSC, Santa Cruz, CA, USA) and A. Spang (Biozentrum, University of Basel, Basel, Switzerland) for sharing antibodies, N. Tavernarakis (Institute of Molecular Biology and Biotechnology, Foundation for Research and Technology-Hellas, Heraklion, Crete, Greece) for sharing the *atg-5* RNAi bacterial clone, X. Wang (State Key Laboratory of Photocatalysis on Energy and Environment, School of Chemistry, Fuzhou University, Fuzhou, China) for the NUC-1::mCherry strain and J. Dumont (Jacques Monod Institute, Paris, France) for the GFP::TBG-1 strain, as well as S. Mitani from the Japanese National Bioresource project for the experimental animal *C. elegans* for providing the *lgg-2* mutants. The LMP-1 monoclonal antibody developed in M.L. Nonet's lab was obtained from the Developmental Studies Hybridoma Bank, created by the NICHD of the National Institutes of Health (NIH) and maintained at The University of Iowa, Department of Biology, Iowa City, USA. Some strains were provided by the CGC, which is funded by NIH Office of Research Infrastructure Programs (P40 OD010440).

Competing interests

The authors declare no competing or financial interests.

Author contributions

V.G. designed the experiments, performed experiments, analyzed the data and wrote the article. A.D., J.L.D. and M.S. designed and performed experiments, analyzed data and read the article. S.A. and C.P. performed experiments, analyzed data and read the article. Y.-Y.L. performed experiments, analyzed data and read the article, and M.R. performed experiments and read the article.

Funding

This study was supported by the Centre National de la Recherche Scientifique (ATIP Grant to V.G.), the Sorbonne University (to V.G.), the Agence Nationale de la Recherche [ANR 07-BLAN-0063-21 and ANR 12-BSV2-0018-01 to V.G.], the Bettencourt-Schueller Foundation [Coups d'élan pour la recherche 2012 to V.G.]; by the ARC Foundation (fellowship to A.D.) and by the French Ministry of Higher Education and Research (fellowship to S.A.).

Supplementary material

Supplementary material available online at
http://dev.biologists.org/lookup/suppl/doi:10.1242/dev.117879/-/DC1

References

Al Rawi, S., Louvet-Vallée, S., Djeddi, A., Sachse, M., Culetto, E., Hajjar, C., Boyd, L., Legouis, R. and Galy, V. (2011). Postfertilization autophagy of sperm organelles prevents paternal mitochondrial DNA transmission. *Science* **334**, 1144-1147.

Alberti, A., Michelet, X., Djeddi, A. and Legouis, R. (2010). The autophagosomal protein LGG-2 acts synergistically with LGG-1 in dauer formation and longevity in C. elegans. *Autophagy* **6**, 622–633.

Askjaer, P., Galy, V. and Meister, P. (2014). Modern tools to study nuclear pore complexes and nucleocytoplasmic transport in Caenorhabditis elegans. *Methods Cell Biol.* **122**, 277-310.

Brenner, S. (1974). The genetics of Caenorhabditis elegans. *Genetics* **77**, 71-94.

Bucci, C., Parton, R. G., Mather, I. H., Stunnenberg, H., Simons, K., Hoflack, B. and Zerial, M. (1992). The small GTPase rab5 functions as a regulatory factor in the early endocytic pathway. *Cell* **70**, 715-728.

Eskelinen, E. L., Reggiori, F., Baba, M., Kovács, A. L. and Seglen, P. O. (2011). Seeing is believing: the impact of electron microscopy on autophagy research. *Autophagy* **7**, 935-956.

Fass, E., Shvets, E., Degani, I., Hirschberg, K. and Elazar, Z. (2006). Microtubules support production of starvation-induced autophagosomes but not their targeting and fusion with lysosomes. *J. Biol. Chem.* **281**, 36303-36316.
Galy, V., Mattaj, I. W. and Askjaer, P. (2003). Caenorhabditis elegans nucleoporins Nup93 and Nup205 determine the limit of nuclear pore complex size exclusion in vivo. *Mol. Biol. Cell* **14**, 5104-5115.
Gönczy, P., Pichler, S., Kirkham, M. and Hyman, A. A. (1999). Cytoplasmic dynein is required for distinct aspects of MTOC positioning, including centrosome separation, in the one cell stage Caenorhabditis elegans embryo. *J. Cell Biol.* **147**, 135-150.
Gorvel, J.-P., Chavrier, P., Zerial, M. and Gruenberg, J. (1991). rab5 controls early endosome fusion in vitro. *Cell* **64**, 915-925.
Hird, S. N. and White, J. G. (1993). Cortical and cytoplasmic flow polarity in early embryonic cells of Caenorhabditis elegans. *J. Cell Biol.* **121**, 1343-1355.
Jahreiss, L., Menzies, F. M. and Rubinsztein, D. C. (2008). The itinerary of autophagosomes: from peripheral formation to kiss-and-run fusion with lysosomes. *Traffic* **9**, 574-587.
Kimura, S., Noda, T. and Yoshimori, T. (2008). Dynein-dependent movement of autophagosomes mediates efficient encounters with lysosomes. *Cell Struct. Funct.* **33**, 109-122.
Klionsky, D. J., Abdalla, F. C., Abeliovich, H., Abraham, R. T., Acevedo-Arozena, A., Adeli, K., Agholme, L., Agnello, M., Agostinis, P., Aguirre-Ghiso, J. A. et al. (2012). Guidelines for the use and interpretation of assays for monitoring autophagy. *Autophagy* **8**, 445-544.
Köchl, R., Hu, X. W., Chan, E. Y. W. and Tooze, S. A. (2006). Microtubules facilitate autophagosome formation and fusion of autophagosomes with endosomes. *Traffic* **7**, 129-145.
Kostich, M., Fire, A. and Fambrough, D. M. (2000). Identification and molecular-genetic characterization of a LAMP/CD68-like protein from Caenorhabditis elegans. *J. Cell Sci.* **113**, 2595-2606.
Kouno, T., Mizuguchi, M., Tanida, I., Ueno, T., Kanematsu, T., Mori, Y., Shinoda, H., Hirata, M., Kominami, E. and Kawano, K. (2005). Solution structure of microtubule-associated protein light chain 3 and identification of its functional subdomains. *J. Biol. Chem.* **280**, 24610-24617.
Kuznetsov, S. A. and Gelfand, V. I. (1987). 18 kDa microtubule-associated protein: identification as a new light chain (LC-3) of microtubule-associated protein 1 (MAP-1). *FEBS Lett.* **212**, 145-148.
Li, W., Zou, W., Yang, Y., Chai, Y., Chen, B., Cheng, S., Tian, D., Wang, X., Vale, R. D. and Ou, G. (2012). Autophagy genes function sequentially to promote apoptotic cell corpse degradation in the engulfing cell. *J. Cell Biol.* **197**, 27-35.
Luo, S.-M., Ge, Z.-J., Wang, Z.-W., Jiang, Z.-Z., Wang, Z.-B., Ouyang, Y.-C., Hou, Y., Schatten, H. and Sun, Q.-Y. (2013a). Unique insights into maternal mitochondrial inheritance in mice. *Proc. Natl. Acad. Sci. USA* **110**, 13038-13043.
Luo, S.-M., Schatten, H. and Sun, Q.-Y. (2013b). Sperm mitochondria in reproduction: good or bad and where do they go? *J. Genet. Genomics* **40**, 549-556.
Maday, S., Wallace, K. E. and Holzbaur, E. L. F. (2012). Autophagosomes initiate distally and mature during transport toward the cell soma in primary neurons. *J. Cell Biol.* **196**, 407-417.
Manil-Ségalen, M., Lefebvre, C., Jenzer, C., Trichet, M., Boulogne, C., Satiat-Jeunemaitre, B. and Legouis, R. (2014). The C. elegans LC3 acts downstream of GABARAP to degrade autophagosomes by interacting with the HOPS subunit VPS39. *Dev. Cell* **28**, 43-55.
Mann, S. S. and Hammarback, J. A. (1994). Molecular characterization of light chain 3. A microtubule binding subunit of MAP1A and MAP1B. *J. Biol. Chem.* **269**, 11492-11497.
Meléndez, A., Tallóczy, Z., Seaman, M., Eskelinen, E. L., Hall, D. H. and Levine, B. (2003). Autophagy genes are essential for dauer development and life-span extension in C. elegans. *Science* **301**, 1387-1391.
Miller, D. M. and Shakes, D. C. (1995). Immunofluorescence microscopy. *Methods Cell Biol.* **48**, 365-394.
Mizushima, N., Yoshimori, T. and Ohsumi, Y. (2011). The role of Atg proteins in autophagosome formation. *Annu. Rev. Cell Dev. Biol.* **27**, 107-132.
Munro, E., Nance, J. and Priess, J. R. (2004). Cortical flows powered by asymmetrical contraction transport PAR proteins to establish and maintain anterior-posterior polarity in the early C. elegans embryo. *Dev. Cell* **7**, 413-424.
Nakatogawa, H., Ichimura, Y. and Ohsumi, Y. (2007). Atg8, a ubiquitin-like protein required for autophagosome formation, mediates membrane tethering and hemifusion. *Cell* **130**, 165-178.
Nielsen, E., Severin, F., Backer, J. M., Hyman, A. A. and Zerial, M. (1999). Rab5 regulates motility of early endosomes on microtubules. *Nat. Cell Biol.* **1**, 376-382.
Politi, Y., Gal, L., Kalifa, Y., Ravid, L., Elazar, Z. and Arama, E. (2014). Paternal mitochondrial destruction after fertilization is mediated by a common endocytic and autophagic pathway in Drosophila. *Dev. Cell* **29**, 305-320.
Ravikumar, B., Acevedo-Arozena, A., Imarisio, S., Berger, Z., Vacher, C., O'Kane, C. J., Brown, S. D. and Rubinsztein, D. C. (2005). Dynein mutations impair autophagic clearance of aggregate-prone proteins. *Nat. Genet.* **37**, 771-776.
Rink, J., Ghigo, E., Kalaidzidis, Y. and Zerial, M. (2005). Rab conversion as a mechanism of progression from early to late endosomes. *Cell* **122**, 735-749.
Sato, M. and Sato, K. (2011). Degradation of paternal mitochondria by fertilization-triggered autophagy in C. elegans embryos. *Science* **334**, 1141-1144.
Seidel, H. S., Ailion, M., Li, J., van Oudenaarden, A., Rockman, M. V. and Kruglyak, L. (2011). A novel sperm-delivered toxin causes late-stage embryo lethality and transmission ratio distortion in C. elegans. *PLoS Biol.* **9**, e1001115.
Sönnichsen, B., Koski, L. B., Walsh, A., Marschall, P., Neumann, B., Brehm, M., Alleaume, A.-M., Artelt, J., Bettencourt, P., Cassin, E. et al. (2005). Full-genome RNAi profiling of early embryogenesis in Caenorhabditis elegans. *Nature* **434**, 462-469.
Strome, S. (1986). Fluorescence visualization of the distribution of microfilaments in gonads and early embryos of the nematode Caenorhabditis elegans. *J. Cell Biol.* **103**, 2241-2252.
Sun-Wada, G.-H., Tabata, H., Kawamura, N., Aoyama, M. and Wada, Y. (2009). Direct recruitment of H+-ATPase from lysosomes for phagosomal acidification. *J. Cell Sci.* **122**, 2504-2513.
Tanida, I., Minematsu-Ikeguchi, N., Ueno, T. and Kominami, E. (2005). Lysosomal turnover, but not a cellular level, of endogenous LC3 is a marker for autophagy. *Autophagy* **1**, 84-91.
Wu, Y. C., Stanfield, G. M. and Horvitz, H. R. (2000). NUC-1, a caenorhabditis elegans DNase II homolog, functions in an intermediate step of DNA degradation during apoptosis. *Genes Dev.* **14**, 536-548.
Zhang, Y., Yan, L., Zhou, Z., Yang, P., Tian, E., Zhang, K., Zhao, Y., Li, Z., Song, B., Han, J. et al. (2009). SEPA-1 mediates the specific recognition and degradation of P granule components by autophagy in C. elegans. *Cell* **136**, 308-321.
Zhou, Q., Li, H. and Xue, D. (2011). Elimination of paternal mitochondria through the lysosomal degradation pathway in C. elegans. *Cell Res.* **21**, 1662-1669.